Bioconjugate Chemistry

pubs.acs.org/bc Article

In Vivo Pretargeting Based on Cysteine-Selective Antibody Modification with IEDDA Bioorthogonal Handles for Click Chemistry

Vera F. C. Ferreira, Bruno L. Oliveira,* Alice D'Onofrio, Carlos M. Farinha, Lurdes Gano, António Paulo, Gonçalo J. L. Bernardes,* and Filipa Mendes*

Cite This: *Bioconjugate Chem.* 2021, 32, 121−132 Read Online

ACCESS | Metrics & More | Article Recommendations | Supporting Information

ABSTRACT: Pretargeted imaging has emerged as an effective multistep strategy aiming to improve imaging contrast and reduce patient radiation exposure through decoupling of the radioactivity from the targeting vector. The inverse electron-demand Diels−Alder (IEDDA) reaction between a *trans*-cyclooctene (TCO)-conjugated antibody and a labeled tetrazine holds great promise for pretargeted imaging applications due to its bioorthogonality, rapid kinetics under mild conditions, and formation of stable products. Herein, we describe the use of functionalized carbonylacrylic reagents for site-specific incorporation of TCO onto a human epidermal growth factor receptor 2 (HER2) antibody (THIOMAB) containing an engineered unpaired cysteine residue, generating homogeneous conjugates. Precise labeling of THIOMAB−TCO with a fluorescent or radiolabeled tetrazine revealed the potential of the TCO-functionalized antibody for imaging the HER2 after pretargeting in a cellular context in a HER2 positive breast cancer cell line. Control studies with MDA−MD-231 cells, which do not express HER2, further confirmed the target specificity of the modified antibody. THIOMAB−TCO was also evaluated in vivo after pretargeting and subsequent administration of an ^{111}In-labeled tetrazine. Biodistribution studies in breast cancer tumor-bearing mice showed a significant activity accumulation on HER2$^+$ tumors, which was 2.6-fold higher than in HER2$^-$ tumors. Additionally, biodistribution studies with THIOMAB without the TCO handle also resulted in a decreased uptake of ^{111}In−DOTA−Tz on HER2$^+$ tumors. Altogether, these results clearly indicate the occurrence of the click reaction at the tumor site, i.e., pretargeting of SK-BR-3 HER2-expressing cells with THIOMAB−TCO and reaction through the TCO moiety present in the antibody. The combined advantages of site-selectivity and stability of TCO tagged-antibodies could allow application of biorthogonal chemistry strategies for pretargeting imaging with minimal side-reactions and background.

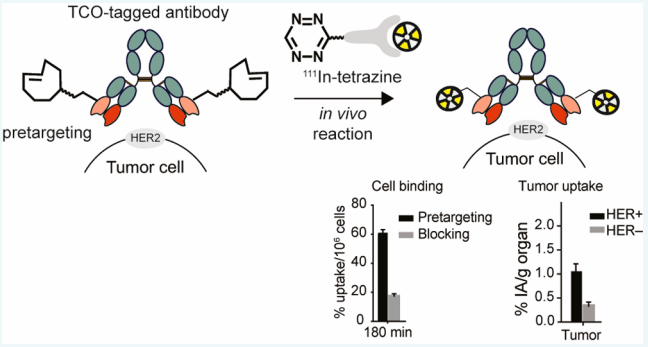

INTRODUCTION

Specific binding of antibodies to a given target with nano- or picomolar affinity has provided the basis for developing highly sensitive, antibody-based imaging agents to assess disease in preclinical and clinical studies. Indeed, there are currently over 30 clinical trials evaluating the utility of immuno-nuclear imaging agents in multiple cancer types.[1,2]

However, despite their attractive properties, antibodies present a few limitations that may hamper their use as imaging agents, namely a long serum half-life (1−3 weeks).[3] As several days are required to achieve high imaging contrast, antibodies are commonly labeled with long-lived radionuclides, such as zirconium-89 (^{89}Zr, $t_{1/2}$ = 78.4 h), copper-64 (^{64}Cu, $t_{1/2}$ = 12.7 h), iodine-124 (^{124}I, $t_{1/2}$ = 100.3 h), and yttrium-86 (^{86}Y, $t_{1/2}$ = 14.7 h),[4] translating in prolonged patient radiation exposure.[3]

An alternative approach has arisen with the development of the pretargeting strategy, based on the decoupling of the radioactivity from the targeting vector.[5,6] This strategy relies on the combination of two components, a targeting vector and a posteriorly administrated, low molecular weight radioligand which leads to in vivo radiolabeling. The pretargeting strategy combines the high affinity and specificity of the vector, usually antibody-based, to the target, and the superior pharmacokinetic properties of the radioligand. The separate administration of the targeting vector and radioligand allows the use of short-lived radionuclides, reduces the patient radiation exposure with minimization of the radiation dose delivered to nontarget organs and tissues, and improves the imaging contrast at earlier time points.[7,8]

Bioorthogonal reactions have emerged as promising tools to selectively modify biological molecules to investigate cellular

Received: October 2, 2020
Revised: November 23, 2020
Published: December 9, 2020

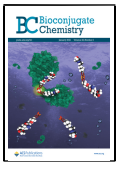

https://dx.doi.org/10.1021/acs.bioconjchem.0c00551
Bioconjugate Chem. 2021, 32, 121−132

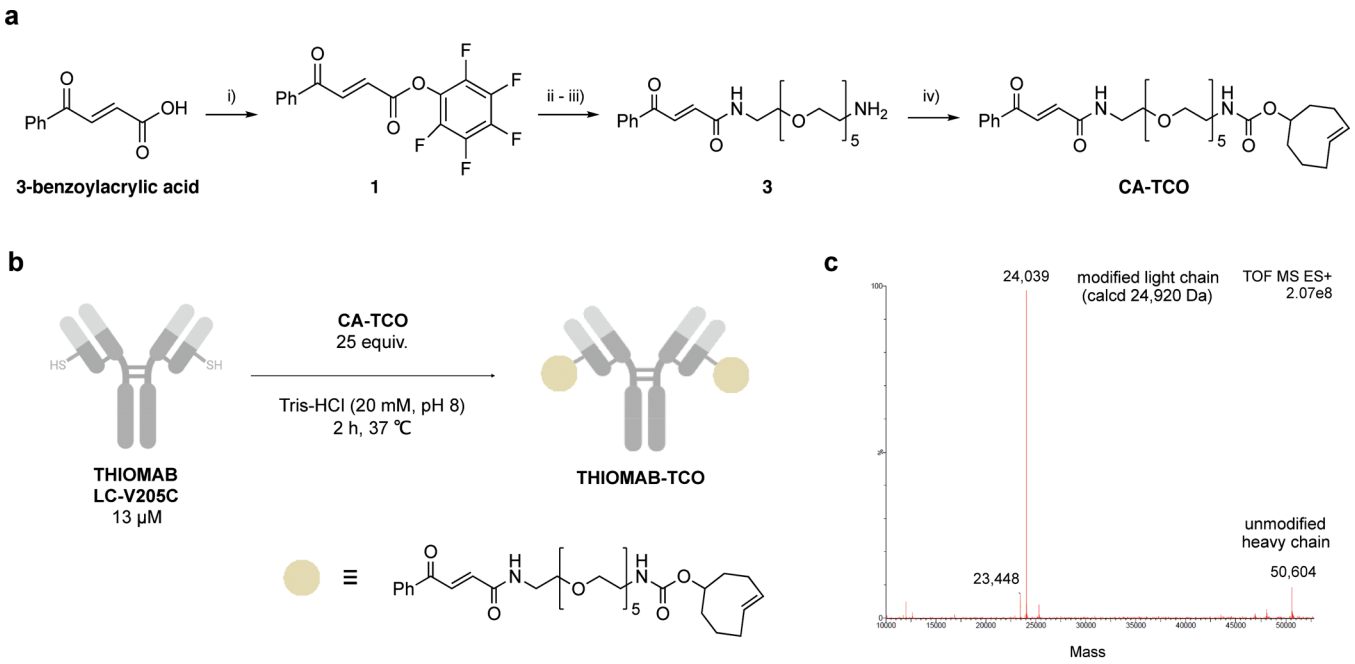

Figure 1. Carbonylacrylic−TCO reagent for antibody modification. (a) Synthesis of carbonylacrylic derivative functionalized with TCO. (i) 3-benzoylacrylic acid, 1.1 equiv pentafluorophenyl trifluoroacetate, 2 equiv DIPEA, anhydrous DCM, RT, 2 h, η = 68.4%; (ii) 1.1 equiv *t*Bu-NH-PEG_5-$(CH_2)_2$-NH_2, 2 equiv DIPEA, anhydrous DCM, RT, 1 h, η = 82.9%; (iii) TFA, DCM, RT, 1 h; and (iv) TCO-NHS-ester, 1.5 equiv **3**, 2 equiv DIPEA, anhydrous DCM, RT, overnight, η = 50.6%. Ph−phenol; (b) schematic overview of antibody modification via reaction with **CA−TCO** (2 h at 37 °C in Tris-HCl buffer); and (c) ESI−MS spectrum of THIOMAB after reaction with **CA−TCO**.

functions and dynamic processes in living systems without interfering with those processes.[9,10] One of the most developed applications of bioorthogonal reactions has been in the pretargeted imaging through the assembly of molecular imaging agents in vivo.[11] To date, the inverse electron-demand [4 + 2] Diels−Alder (IEDDA) cycloaddition, between a 1,2,4,5-tetrazine and strained alkene dienophile, is considered the most suitable click reaction to pretargeted imaging applications, as it presents high selectivity and fast kinetics, proceeds in mild conditions, and is catalyst-free.[12] The IEDDA reaction has been applied in in vivo pretargeted imaging using a variety of radionuclides, such as technetium-99m (^{99m}Tc, $t_{1/2}$ = 6.0 h),[13] indium-111 (^{111}In, $t_{1/2}$ = 67.2 h),[14,15] copper-64 (^{64}Cu, $t_{1/2}$ = 12.7 h),[16−18] fluorine-18 (^{18}F, $t_{1/2}$ = 109.8 min),[19−21] and gallium-68 (^{68}Ga, $t_{1/2}$ = 68.0 min).[22−24]

Conjugation of IEDDA reactant moieties to antibodies usually relies on amine-reactive *N*-hydroxysuccinimide (NHS) esters for covalent binding.[15] This strategy leads to random conjugation of IEDDA partners to lysine residues resulting in heterogeneous conjugates with undefined composition, which can substantially lower the bioactivity of the modified protein and lead to unpredictable in vivo behavior. It is therefore critical to establish a well-defined conjugation strategy for antibody modification to ensure that both targeting and pharmacokinetics are maintained.

Site-selective protein modification methods have been crucial for the development of new biologically active protein conjugates for in vivo applications.[25] From all the natural amino acids, cysteine is considered the ideal amino acid for selective protein modification due to its low abundance and the high nucleophilicity of the sulfhydryl side chain.[26,27] Maleimides are still the most commonly used reagents for cysteine bioconjugation. These reagents present fast reaction kinetics in aqueous media and are easy to chemically modify. However, it is known that the thio-succinimidyl conjugates formed are unstable and react with thiols present in plasma, leading to maleimide release.[28−30]

Recently, we reported a new methodology for irreversible cysteine-selective protein bioconjugation via carbonylacrylic reagents.[31,32] These easily prepared reagents are highly reactive for cysteine in aqueous conditions at near neutral pH and using stoichiometric amounts, and form stable products that remain biologically functional. The aforementioned characteristics in combination with the availability of biologically relevant cysteine-tagged proteins make this method suitable for routine preparation of well-defined and stable conjugates for chemical biology applications.

Herein, a novel carbonylacrylic derivative functionalized with a *trans*-cyclooctene (TCO) moiety was developed and conjugated to THIOMAB LC-V205C, a modified trastuzumab antibody against the human epidermal growth factor receptor 2 (HER2) presenting an engineered cysteine in the light chain.[33] This receptor has already been exploited in clinical imaging of breast and gastric cancer HER2-expressing tumors.[14,19,20,34−40] Pretargeting was first explored in vitro to assess the IEDDA reaction between the antibody bound to HER2-expressing cells and a fluorescent/radiolabeled tetrazine. Then, in vivo studies were performed in a relevant HER2$^+$ mouse model using an ^{111}In-labeled tetrazine. This approach represents the first maleimide-free methodology for cysteine-based incorporation of TCO onto antibodies for IEDDA pretargeting approaches.

CYSTEINE-SELECTIVE ANTIBODY MODIFICATION

A TCO-functionalized carbonylacrylic reagent for cysteine-antibody modification was synthesized as depicted in Figure 1. Activation of the commercially available 3-benzoylacrylic acid was performed using pentafluorophenyl trifluoroacetate as activating agent to give compound **1** (Figure 1a i). Subsequent

https://dx.doi.org/10.1021/acs.bioconjchem.0c00551
Bioconjugate Chem. 2021, 32, 121−132

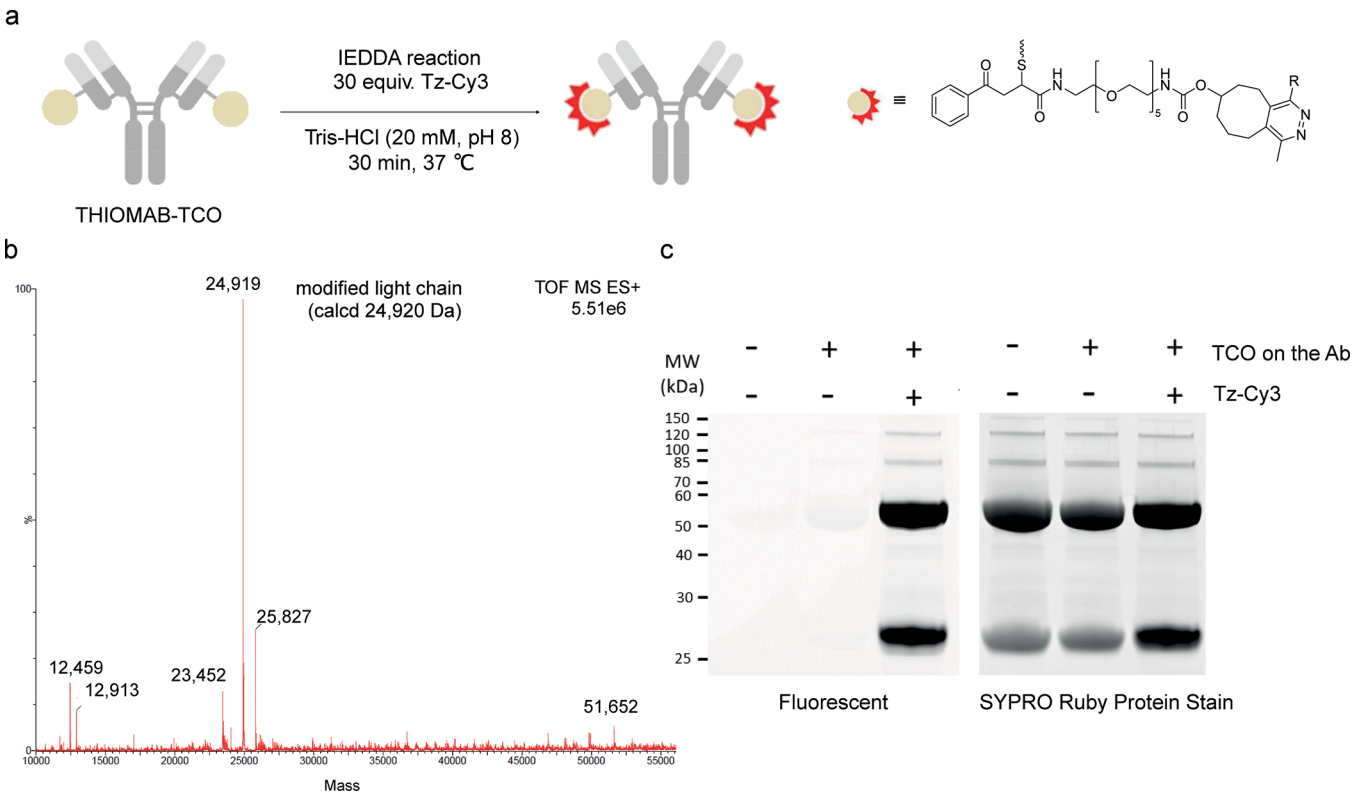

Figure 2. Fluorescent labeling studies of THIOMAB-TCO. (a) Schematic overview of antibody labeling via click reaction with 6-methyl-tetrazine-sulfo-Cy3 (Tz−Cy3); (b) ESI−MS spectrum of THIOMAB−TCO after reaction with fluorescent tetrazine (30 min at 37 °C in Tris-HCl buffer); and (c) SDS-PAGE analysis of fluorescent labeling of THIOMAB−TCO conjugate. Proteins were resolved in a 4−12% gradient NuPAGE Bis-Tris mini gel under reducing conditions, and revealed using SYPRO Ruby staining.

introduction of a short polyethylene glycol (PEG) linker to increase hydrophilicity was accomplished by reacting precursor **1** with *t*Bu-NH−PEG_5−$(CH_2)_2$−NH_2, followed by *tert*-butyl deprotection with trifluoroacetic acid (TFA) (Figure 1a ii,iii). Finally, reaction of the PEGylated compound **3** with the commercially available TCO−NHS−ester yielded the water-soluble, TCO-functionalized reagent **CA−TCO** (carbonylacrylic-TCO), with an overall yield of ∼28% (Figures 1a iv and S1−S3 of the Supporting Information, SI).

The efficacy of **CA−TCO** for site-selective protein modification was tested using the anti-HER2 antibody THIOMAB LC-V205C.[33] Bioconjugation proceeded to completion (>95%) upon reaction with 25 equiv of **CA−TCO** for 2 h at 37 °C (Figure 1b). The antibody was treated with the reducing agent tris(2-carboxyethyl)phosphine (TCEP) prior to mass spectrometry analysis to reduce the interchain disulfide bridges, yielding the light and heavy chains. Liquid chromatography−mass spectrometry (LC−MS) analysis after TCEP reduction showed a single modification in the light chain, while the heavy chain remained unmodified (Figures 1c and S4−S6), resulting in two TCO molecules per each THIOMAB molecule. This result demonstrates that the IEDDA-functionalized carbonylacrylic reagent retains the selectivity for cysteine, and therefore can be used for site-selective modification of proteins of interest.

PRECISE ANTIBODY FLUORESCENT LABELING

To demonstrate the applicability of the TCO-functionalized carbonylacrylic reagent to fluorescently label proteins, the THIOMAB−TCO conjugate was reacted with a fluorescent (Tz−Cy3, Figures 2a and S7) and nonfluorescent (benzylamino methyl-tetrazine, Figure S8) tetrazine. Mass spectrometry analysis indicated complete conversion of THIOMAB−TCO to the corresponding antibody conjugates (Figures 2 and S6) resulting in the incorporation of two tetrazine moieties per antibody. SDS-PAGE in-gel fluorescence analysis of the reaction revealed fluorescent labeling by click reaction between the TCO moiety present in each light chain of the antibody and the fluorescent tetrazine, indicated by the ∼25 kDa fluorescent band (Figure 2c). A fluorescent band of ∼50 kDa was also observed, that might correspond to the formation of a dimer between the modified light chains, as there was no indication of conjugation to the heavy chain (∼50 kDa) by mass spectrometry. In fact, dimerization of the light chains was also observed by LC−MS analysis performed under strong denaturing conditions (i.e., TCEP reduction, acetonitrile as running solvent, desolvation temperature 400 °C, Figures S7 and S8). Importantly, nonspecific binding of the tetrazine fluorophore to the heavy chain was also not observed by SDS-PAGE (Figure S9).

IN VITRO CELLULAR PRETARGETING VIA CLICK REACTION OF ANTIBODY CONJUGATE WITH A FLUORESCENT IEDDA PARTNER

Having proven the efficacy of the TCO-functionalized carbonylacrylic derivative to create a precisely modified, fluorescently labeled antibody through TCO-functionalization, the next step was to assess if the antibody conjugate could be used in a pretargeting approach. With this purpose, the human breast cancer SK−BR-3 cells ($HER2^+$, 3^+ immunohistochem-

https://dx.doi.org/10.1021/acs.bioconjchem.0c00551
Bioconjugate Chem. 2021, 32, 121−132

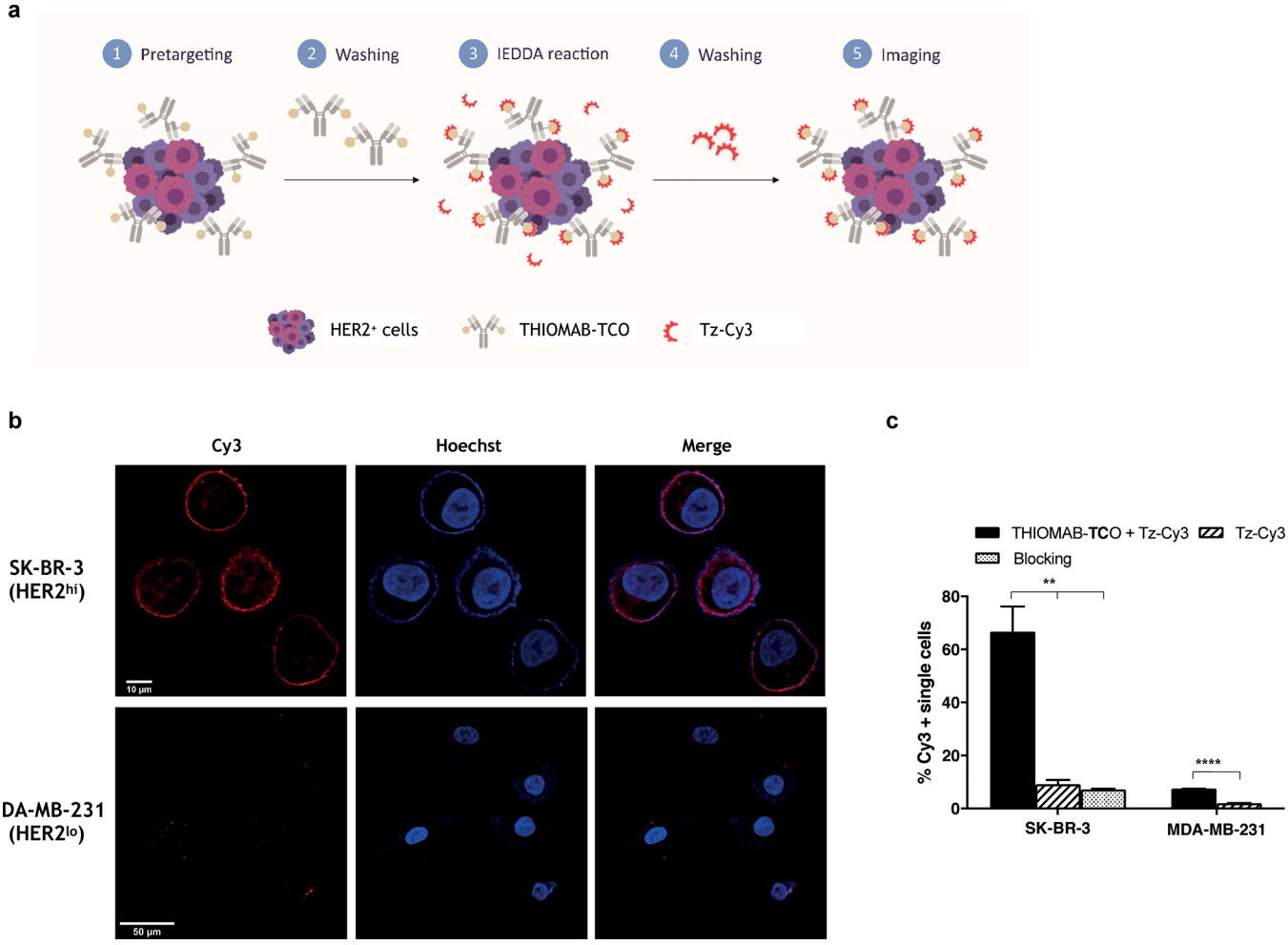

Figure 3. Pretargeted cell labeling with THIOMAB−TCO. (a) Schematic overview of pretargeting strategy; (b) confocal images of SK−BR-3 and MDA−MB-231 cells pretargeted with THIOMAB−TCO for 45 min at 37 °C followed by treatment with Tz−Cy3 for 30 min at 37 °C. Nuclei are shown in blue. Experiments performed in triplicate; (c) percentage of Cy3-positive single cells from the cell population in SK−BR-3 and MDA−MB-231 cells treated with THIOMAB−TCO (45 min, RT), blocking with THIOMAB (45 min, RT) before THIOMAB−TCO, followed by treatment with Tz−Cy3 (30 min, 37 °C), and Tz−Cy3 only. Statistical analysis was performed with two-way ANOVA, with a p-value <0.05 considered as the level of statistical significance.

istry (IHC) score) and the triple-negative MDA−MB-231 (HER2-) cells[41] were pretargeted with THIOMAB−TCO followed by treatment with the fluorescent tetrazine Tz−Cy3 (Figure 3a). HER2 visualization at the plasma membrane of SK−BR-3 cells through confocal microscopy indicated successful click reaction between the TCO moiety present on THIOMAB−TCO and the fluorescent tetrazine in cell medium, evidencing the bioorthogonality of the IEDDA reaction (Figure 3b). Importantly, no fluorescent signal was detected at the plasma membrane of SK−BR-3 cells treated with tetrazine only and pretargeted with the unmodified THIOMAB (Figure S10).

These results clearly indicate that the fluorescent signal is associated with the labeling of the antibody via TCO. Lastly, confocal imaging of the HER2- cell line further support labeling of the HER2 receptor, as no fluorescence was detected at the cell surface of MDA−MB-231 cells treated with THIOMAB−TCO followed by Tz−Cy3 (Figure 3b). Staining of SK−BR-3 cells treated with THIOMAB−TCO was also observed by flow cytometry after reaction with Tz−Cy3 (Figures 3c and S11), confirming IEDDA reaction between the TCO moiety present in THIOMAB−TCO and tetrazine. Cell staining was antibody-associated, as shown by the low unspecific binding of Tz−Cy3 to SK−BR-3 cells (~10%). Blocking of HER2 receptors with unmodified THIOMAB before incubation with THIOMAB−TCO led to a decrease in the fluorescence intensity observed in SK−BR-3 cells (~7% binding after blocking), supporting that THIOMAB−TCO retained its specificity for HER2. The high percentage of stained SK−BR-3 cells (~73%) vs stained MDA−MB-231 cells (~8%) further indicated that binding of THIOMAB−TCO was specific for HER2.

Altogether, the results obtained by confocal microscopy and flow cytometry demonstrate in vitro pretargeting of HER2-expressing cells with THIOMAB−TCO in a cellular context. Moreover, the results also indicate that the THIOMAB−TCO conjugate retained the specificity for its target after TCO functionalization, being able to detect HER2 at the surface of HER2-expressing cells after local reaction with a fluorescent tetrazine.

■ PRECISE ANTIBODY RADIOLABELING

Considering the successful in vitro pretargeting of HER2-expressing cells, the work proceeded with the study of

https://dx.doi.org/10.1021/acs.bioconjchem.0c00551
Bioconjugate Chem. 2021, 32, 121−132

THIOMAB−TCO for in vivo pretargeting through IEDDA reaction with a radiolabeled tetrazine. With this purpose, the chelating agent 1,4,7,10-tetraazacyclododecane-1,4,7,10-tetraacetic acid (DOTA) functionalized with a tetrazine moiety[42] was labeled with ^{111}In by reaction with $^{111}InCl_3$ for 15 min at 80 °C in 0.1 M ammonium acetate buffer pH 7 (Figure 4a).

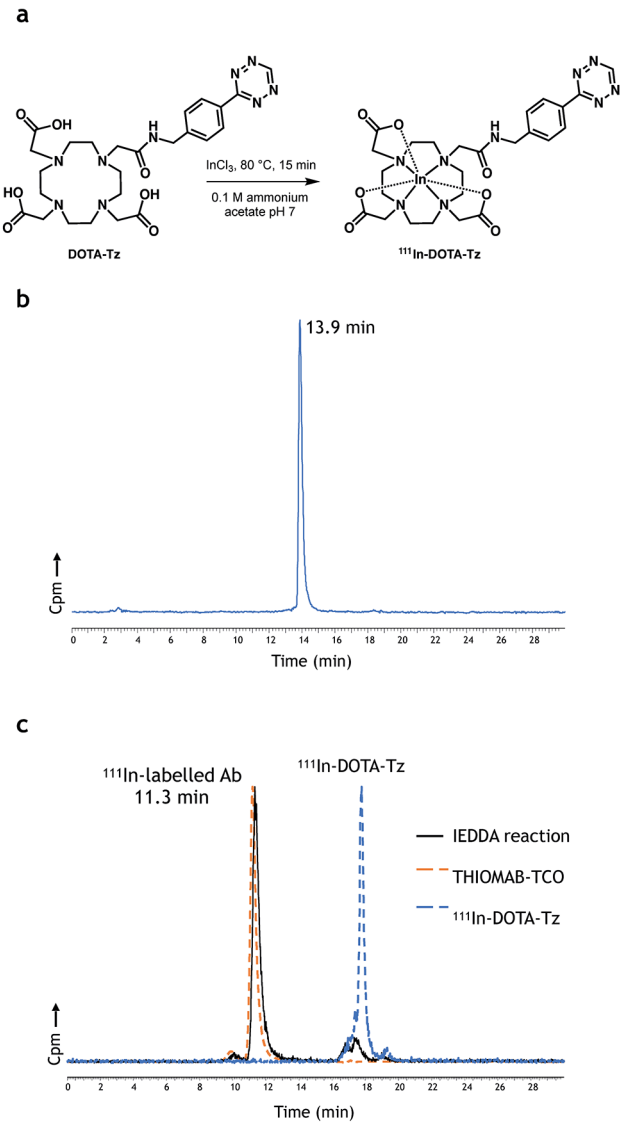

Figure 4. Radiolabeling of THIOMAB−TCO. (a) Labeling of DOTA−Tz ([1 × 10^{-4} M]) with ^{111}In for 15 min at 80 °C; (b) characterization of ^{111}In−DOTA−Tz by RP−HPLC after purification; (c) SE−HPLC analysis of IEDDA reaction of THIOMAB−TCO with ^{111}In−DOTA−Tz for 5 min at 37 °C (black line, γ-detection). Orange dashed line represents analysis of THIOMAB−TCO (UV detection) and blue dashed line analysis of ^{111}In−DOTA−Tz (γ-detection). Cpm—counts per minute.

After HPLC purification, ^{111}In−DOTA−Tz was isolated with a radiochemical purity (RCP) > 95% and a radiochemical yield (RCY) ranging from 44 to 56% (Figure 4b). Analysis by instant thin layer chromatography (iTLC) discarded the formation of indium colloids (Figure S12). THIOMAB−TCO was then radiolabeled by click reaction with the purified ^{111}In−DOTA−Tz for 5 min at 37 °C, with ∼92% of the activity being associated with the clicked antibody (Figure 4c) (RCP > 99% after purification, Figure S13). These results further confirm the fast kinetics and high efficiency of the biorthogonal reaction, as both partners were used at very low concentration, in the micromolar range.

The ^{111}In-labeled antibody remained fully stable in cell culture medium and was totally resistant to transchelation in the presence of the ^{111}In chelating agent diethylenetriamine pentaacetic acid (DTPA, incubation at 37 °C for 3 h, Figure S14). Finally, in human serum, a time-dependent decrease in the radiochemical stability of the tetrazine−TCO antibody was observed (∼54% of RCP after 24 h of incubation at 37 °C) (Figure S15).

IN VITRO PRETARGETING OF HER2-POSITIVE CELLS FOR HER2 IMAGING

Having proven the ability to rapidly radiolabel THIOMAB−TCO with ^{111}In in mild conditions through the IEDDA reaction, an in vitro pretargeting approach was explored. HER2$^+$ and HER2$^-$ cells were pretargeted with THIOMAB−TCO followed by treatment with ^{111}In−DOTA−Tz (Figure 5a). Low unspecific binding of the radiolabeled tetrazine was observed for SK−BR-3 cells (0.1−0.2%).

Click reaction between HER2-bound THIOMAB−TCO and ^{111}In−DOTA−Tz was observed in SK−BR-3 cells after 10 min of incubation with the radiolabeled tetrazine, with a significantly higher uptake in SK−BR-3 cells when compared to controls (e.g., bound activity to MDA−MB-231, Figure 5a, p-value <0.0001).

Similarly, as previously observed for the fluorescent tetrazine, blocking of HER2 receptors with unmodified THIOMAB (Figure 5b) resulted in a 3.7-fold decrease in the uptake of pretargeted SK−BR-3 cells at 180 min of incubation (p-value <0.0001). It is worth mentioning that a significant time-dependent increase of the uptake in the pretargeted SK−BR-3 cells was observed after 30 min of incubation. This behavior was also observed in SK−BR-3 cells treated with the already clicked antibody, which was allowed to bind to HER2 over time (Figure S16). Considering that the click reaction occurs within 5 min of incubation in cell medium, the increase in the uptake over time might be explained not by a late click reaction, but by internalization of the THIOMAB−TCO−HER2 complexes and posterior recycling to the membrane, where THIOMAB−TCO is again available to react with free ^{111}In−DOTA−Tz present in the assay medium. This hypothesis is supported by confocal immunofluorescence microscopy studies in SK−BR-3 cells in which the internalized trastuzumab was detected after 3 h at 37 °C.[43] Additionally, a recent study demonstrated that trastuzumab−HER2 complexes internalize both in HER2$^{high\ level}$ and HER2$^{low\ level}$ cells, but present distinct postendocytic trafficking behavior, dependent on the expression levels of HER2.[44] In HER2^{hi} cells, internalized trastuzumab traffics to early endosomes and remains on the limiting endosomal membrane, while an only small fraction of antibody−HER2 complexes enters the lysosomal pathway. The trastuzumab is then expected to be segregated from these endosomes into the endocytic recycling pathway.[44] By contrast, in HER2^{lo} cells, internalized antibody−HER2 complexes enter the lysosomal pathway, as there is no evidence of trastuzumab recycling to the membrane.[44] The uptake results obtained in pretargeted MDA−MB-231 cells are also in agreement with the proposed trafficking model. Internalization and lysossomal degradation of THIOMAB−

https://dx.doi.org/10.1021/acs.bioconjchem.0c00551
Bioconjugate Chem. 2021, 32, 121−132

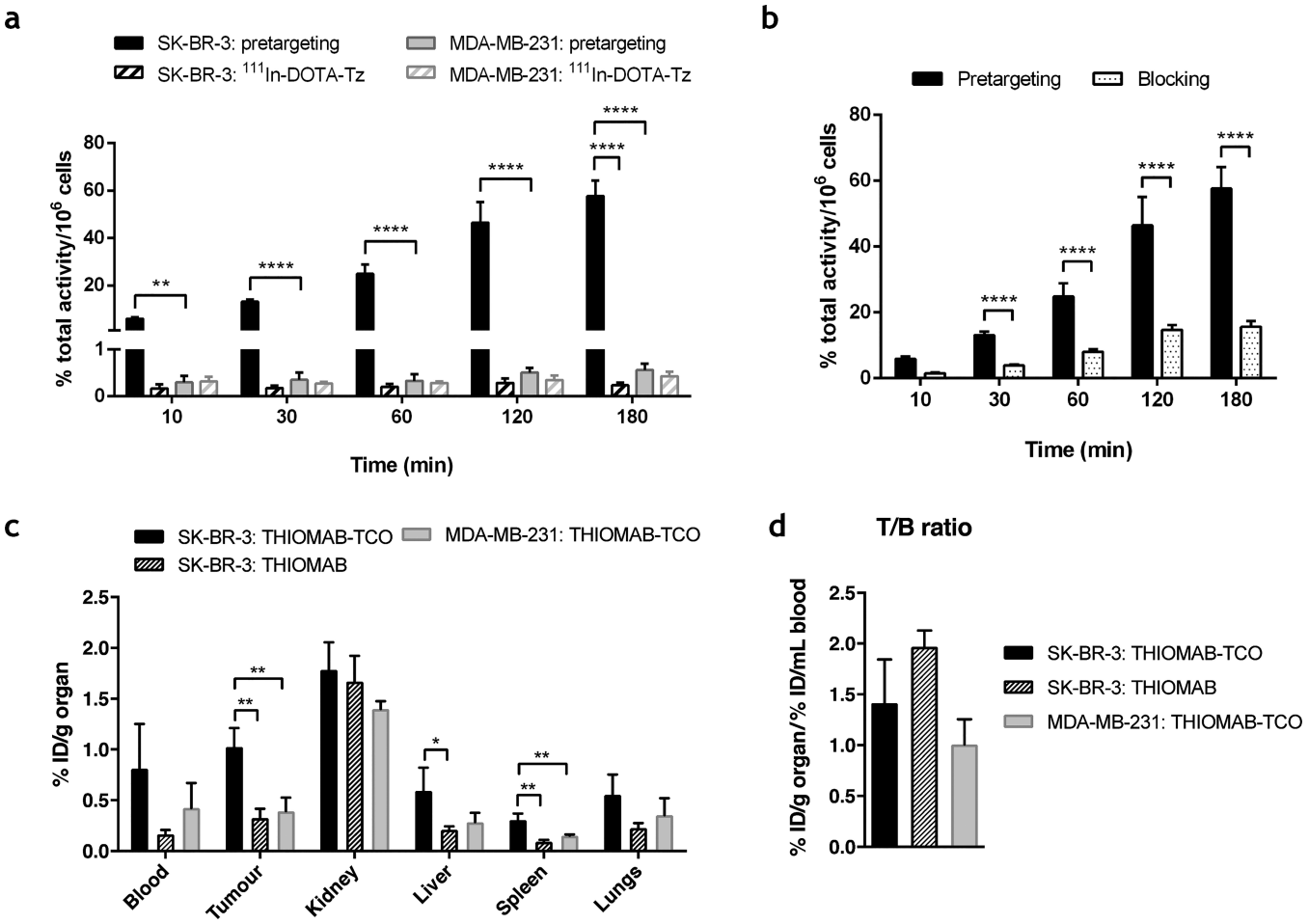

Figure 5. In vitro and in vivo pretargeting. (a) In vitro click reaction of THIOMAB−TCO with ^{111}In−DOTA−Tz in SK−BR-3 and MDA−MB-231 cells. Cells were pretargeted with THIOMAB−TCO for 45 min at 37 °C. The medium containing the antibody−TCO was removed at different time points and cells incubated with ^{111}In−DOTA−Tz at 37 °C. For the control experiment, cells were incubated with ^{111}In−DOTA−Tz only. (b) Blocking of SK−BR-3 cells with THIOMAB (45 min, 37 °C) before pretargeting. Cellular uptake values are expressed as a percentage of total activity added to cells normalized per million of cells ± standard deviation (two independent assays with n = 3−4 replicates for each time point). Statistical analysis was performed with two-way ANOVA, with p-value <0.05 considered as the level of statistical significance. (c) Biodistribution (% ID/g) in the most relevant organs of ^{111}In−DOTA−Tz administered after pretargeting with THIOMAB−TCO, in female athymic nude mice (n = 3 for each group), 24 h post injection of ^{111}In−DOTA−Tz (48 h after antibody injection). Statistical analysis was performed with two-way ANOVA, with p-value <0.05 considered as the level of statistical significance. (d) Tumor-to-blood ratios (%ID/g organ/% ID/mL blood) of SK−BR-3 and MDA−MB-231 tumor-bearing mice receiving THIOMAB−TCO or THIOMAB, 24 h post injection of ^{111}In−DOTA−Tz (48 h after antibody injection). ID/g refers to injected dose/gram.

TCO−HER2 complexes might have diminished the THIOMAB−TCO available to react with ^{111}In−DOTA−Tz, which was reflected in a similar percentage of cell-bound activity over time (0.3% ± 0.1 at 5 min vs 0.6% ± 0.1 at 180 min), comparable to the unspecific binding of the radiolabeled tetrazine (0.3 ± 0.1 at 5 min vs 0.4% ± 0.1 at 180 min).

IN VIVO PRETARGETING OF HER2-POSITIVE TUMORS

We next evaluated the pretargeting strategy using a human HER2 tumor xenograft mouse model. Biodistribution of ^{111}In−DOTA−Tz was assessed after pretargeting with THIOMAB−TCO followed by intravenous injection of ^{111}In−DOTA−Tz 24 h later. Biodistribution in the organs was evaluated at 24 h postinjection of the tetrazine radiocomplex (Figure 5c,d).

The tumoral uptake in SK−BR-3 tumor bearing mice receiving THIOMAB−TCO was significantly higher when compared to control studies (1.02% vs 0.39% and 0.33% of injected dose (ID)/g for unmodified THIOMAB in SK−BR-3 xenografts and for THIOMAB−TCO in MDA−MB-231 xenografts respectively, p-value <0.01). These results clearly indicate click reaction at the tumor site, i.e., pretargeting of HER2$^+$ cells with THIOMAB−TCO and reaction with ^{111}In−DOTA−Tz through the TCO moiety present in the antibody.

In the overall biodistribution profile, it is clear that the majority of the activity was excreted 24 h post injection of ^{111}In−DOTA−Tz, with values ranging from 89.5 to 93.7% ID (Table S1 and Figure S17). Unlike small molecules, antibodies are too large to be filtered by the kidneys and are not eliminated in the urine. In fact, biodistribution of ^{111}In−DOTA−Tz in normal mice revealed an excretion rate of 91.8% ± 1.0 at 1 h after injection.[42] Hence, the high excretion rate obtained with the pretargeting strategy is in agreement with the observed fast elimination of the hydrophilic ^{111}In−DOTA−Tz, which accumulated in the kidneys with values between 1.40−1.79% ID/g for the three groups of mice (Figure 5c), supporting its elimination through the renal

https://dx.doi.org/10.1021/acs.bioconjchem.0c00551
Bioconjugate Chem. 2021, 32, 121−132

pathway. The rapid elimination of ^{111}In−DOTA−Tz is also reflected in low uptake values in the main organs and tissues. Renal excretion was significantly lower in SK−BR-3 mice receiving THIOMAB−TCO compared with mice treated with unmodified THIOMAB (89.5 vs 93.7% ID, p-value <0.01, Figure S17), while accumulation in tumor, blood, and remaining organs was higher for THIOMAB−TCO. The activity found in the liver (0.21−0.59% ID/g) represents the contribution of the hepatobiliary excretion pathway, probably associated with the excretion of the clicked radiolabeled antibody.

Higher activities were observed in the blood of SK−BR-3 and MDA−MB-231 tumor-bearing mice receiving THIOMAB−TCO comparing with mice receiving the unmodified THIOMAB (0.81−0.42% vs 0.17% ID/g, respectively) (Figure 5c). This difference might be associated with systemic retention of the clicked antibody. Indeed, it is well-known that antibodies exhibit a relatively fast distribution phase followed by a slower elimination phase, contributing to long serum half-lives.[45] This biphasic pharmacokinetic profile might explain that, after 48 h of antibody injection, THIOMAB−TCO remained in circulation available for click reaction with ^{111}In−DOTA−Tz. The unmodified THIOMAB was also possibly in circulation, but unable to undergo systemic click reaction due to the absence of a TCO moiety. The possibility of HER2 shedding into systemic circulation is also not discarded.

The Tumor/Blood ratios (T/B ratios) of the three mice groups ranged from 1.0 to 2.0 (Figure 5d). Overall, the higher systemic retention of the clicked antibody contributed to the relatively low T/B ratio observed in SK-BR-3 mice treated with THIOMAB−TCO (∼1.4). In contrast, although the tumor uptake was lower in SK−BR-3 mice receiving THIOMAB, the absence of the TCO moiety in the antibody contributed also to a lower activity in the blood, increasing the T/B ratio to ∼2.0. Therefore, optimization is required to reduce the antibody blood concentration, possibly through the use of clearing agents prior to administration of the radiolabeled tetrazine.[46,47]

In a recent study, the pretargeting of HER2-expressing tumors was exploited through click reaction between THIOMAB antibodies containing different molar ratios of TCO moieties incorporated via maleimide chemistry.[14] At 24 h post ^{111}In−DOTA−Tz injection, the tumoral uptake in KPL-4 (HER2$^+$) tumor-bearing mice was 2% ID/g, ∼2-fold higher than that obtained in this study, at the same antibody concentration (5 mg/kg) and using comparable injected doses (∼3.5 MBq of ^{111}In−DOTA−Tz in this study vs 18.5 MBq). The discrepancy in the tumoral uptake might be related to the different HER2-expressing cell line used.

HER2 is a highly expressed, internalizing target that is passively recycled to the plasma membrane after endocytosis.[44] Internalization of the TCO-modified antibody with its target could constitute a limitation to the pretargeting approach since ^{111}In−DOTA−Tz is not able to cross the cellular membrane due to the polar/charged nature of the metal/chelate moiety. Hence, internalization of THIOMAB−TCO might contribute to the low tumoral uptake in SK−BR-3 tumor-bearing mice, as the HER2−bound antibody was not always available at the cell surface to react with ^{111}In−DOTA−Tz. In fact, the cellular uptake results presented here with pretargeted SK−BR-3 cells support the internalization of THIOMAB−TCO−HER2 complexes, with a subpopulation recycling back to the membrane.

Recently, the bioavailability of HER2 at the cell surface was shown to be modulated through a caveolin 1 (CAV1)-mediated mechanism.[48,49] Indeed, CAV1 depletion by treatment with lovastatin was shown to increase the HER2 half-life and availability at the cell membrane in HER2-positive tumors (e.g., NCIN87 cells). Importantly, the SK−BR-3 cells used in this study do not form caveolae as they lack caveolin 1.[50] The use of a statin, however, might work by modulating other endocytic trafficking systems.[51] Therefore, pharmacological treatment with lovastatin is also envisaged in future biodistribution studies to assess a possible effect on the availability of THIOMAB−TCO to react with ^{111}In−DOTA−Tz.

CONCLUSIONS

New conjugation methods leading to the formation of homogeneous and stable antibody conjugates are still required for pretargeted imaging applications. To our knowledge, this work represents the first maleimide-free methodology for site-specific antibody conjugation of the IEDDA pair for in vivo pretargeted imaging. The IEDDA-functionalized carbonylacrylic derivative proved to be a suitable alternative to the available methods for antibody fluorescence labeling and radiolabeling. This approach is particularly relevant in labeling strategies that require higher temperatures, as is often the case of those involving trivalent radiometals and macrocyclic chelators. By radiolabeling one IEDDA reagent followed by click reaction with an antibody modified in a site-specific way with the corresponding IEDDA partner, this approach allows one to perform room-temperature radiolabeling more rapidly and in higher yield, compared with the traditional "one-pot" methods. Biodistribution results clearly indicate in vivo IEDDA reaction, but optimization is required to improve tumor uptake and tumor-to-background ratios for in vivo imaging.

MATERIALS AND METHODS

General Information. The antibody THIOMAB LC-V205C was provided by Genentech (South San Francisco, CA, U.S.A.). The compound 2,2′,2″-(10-(2-((4-(1,2,4,5-tetrazin-3-yl)benzyl)amino)-2-oxoethyl)-1,4,7,10-tetraazacyclododecane-1,4,7-triyl)triacetic acid (DOTA−Tz) was synthesized as described by D'Onofrio et al.[37] All reagents and solvents used in chemical synthesis were of reagent grade and used without purification. General reagents were purchased from either Sigma-Aldrich or Alfa-Aesar, unless otherwise stated. All cell culture reagents were from Gibco, unless otherwise stated. Analytical thin-layer chromatography (TLC) was carried out on silica gel-coated aluminum plates with fluorescent indicator F254 (Merck). Compounds were detected with UV light (λ = 254 nm), ninhydrin, or potassium permanganate. Compound purification by column chromatography was performed using high-purity grade silica gel (Merck grade 9385) with a pore size of 60 Å and 230−400 mesh particle size.

NMR Spectroscopy. ^{1}H and ^{13}C nuclear magnetic resonance (NMR) spectra were recorded on a 400 MHz DPX-400 Dual Spectrometer (Bruker) in $CDCl_3$ or CD_3OD. ^{1}H and ^{13}C chemical shifts (δ) are reported in parts per million (ppm) and referenced using the residual solvent resonances relative to tetramethylsilane. Signal multiplicity is described using the following abbreviations: s (singlet), d (doublet), t (triplet), and m (multiplet). Characterization of the compounds is described in the SI.

https://dx.doi.org/10.1021/acs.bioconjchem.0c00551
Bioconjugate Chem. 2021, 32, 121−132

Liquid Chromatography–Mass Spectrometry. High-resolution mass determination of small molecules was performed on a Waters LCT Premier spectrometer using ESI ionization and a TOF mass analyzer. 50% (v/v) acetonitrile in bidistilled water with 0.25% (v/v) formic acid was used as mobile phase. LC–MS analysis of small molecules was performed on a Waters SQD2 with Waters H-Class UPLC using ESI ionization (pos/neg switching). Separation was based on a Waters Acquity UPLC BEH C18 column (2.1 × 50 mm^2, 130 Å pore size, 1.7 μm particle size, 0.5 mL/min flow rate, column temperature 37 °C, UV 190–400 nm), using 0.1% (v/v) formic acid in bidistilled water (solvent A) and acetonitrile (solvent B) as mobile phases. Linear gradients of solvents A and B were applied according to the following method: 0–5 min (5–100% B), 5–6.5 min (100% B), and 6.5–8 min (5% B). Protein LC–MS was performed on a Waters Acquity UPLC system equipped with a single quadrupole mass detector. Separation was based on a Waters Acquity Q6 UPLC BEH 300 C4 column (2.1 × 50 mm^2, 300 Å pore size, 1.7 mm particle size, 0.2 mL/min flow rate). Solvents A (0.1% (v/v) formic acid in bidistilled water) and B (71:29:0.075 (v:v) of acetonitrile/bidistilled water/formic acid) were used as mobile phases. The gradient of solvents A and B were applied according to the following method: 0–12 min (28–71.2% A), 12–13 min (71.2–100% A), 13–16 min (100% A), 16–16.5 min (100–28% A), and 16.5–20 min (28% A). The electrospray source was operated with a capillary voltage of 3.0 kV and a cone voltage of 20 V. Nitrogen was used as the desolvation gas at a total flow of 800 L/h with cone volume at 1 L/h. Desolvation temperature was set to 400 °C. Total mass spectra were reconstructed from the ion series using the MaxEnt algorithm preinstalled on MassLynx software (version 4.1 from Waters). To obtain the ion series described, the protein peak(s) of the chromatogram were selected for integration and further analysis.

Radio HPLC Analysis. Radio reversed phase-high performance liquid chromatography (RP–HPLC) analyses were performed on a PerkinElmer Series 200 LC pump (PerkinElmer) coupled to an ultraviolet/visible (UV/vis) detector (Shimadzu SPD-10AV) and to a γ-detector (Berthold-LB 509, Berthold Technologies). Compounds were separated using a Macherey-Nagel EC250/4 Nucleosil 100–10 C18 column (250 × 4 mm^2, 10 Å pore size, 10 μm particle size, 1.0 mL/min flow rate). Linear gradients of eluent A (0.1% (v/v) TFA in bidistilled water) and eluent B (0.1% (v/v) TFA in acetronitrile) were applied according to the following method: 0–5 min (5% B), 5–25 min (5–100% B), 25–26 min (5% B), and 26–30 min (5% B). Elution was monitored via absorbance at 220 nm or γ-detection.

Antibody labeling was monitored by iTLC, using 12.0 × 1.0 cm^2 strips of glass microfiber chromatography paper impregnated with silica gel (Agilent Technologies, Santa Clara, CA, U.S.A.) as stationary phase, and 30% (v/v) methanol in bidistilled water as mobile phase. Activity was detected using the γ-miniGITA TLC scanner (Elysia-raytest). GINA-Star TLC software (Elysia-raytest) allowed for data acquisition and evaluation.

Size exclusion-HPLC (SE-HPLC) analyses were performed on a PerkinElmer Flexar UHPLC System (PerkinElmer) coupled to a Gabi Nova γ-detector (Elysia-raytest). Compounds were separated using a Waters XBridge Protein BEH SEC column (300 × 7.8 mm^2, 200 Å pore size, 3.5 μm particle size, 0.7 mL/min flow rate). Isocratic elution was performed using 0.1 M phosphate buffer pH 6.5 as mobile phase. Elution was monitored via absorbance at 220/280 nm or γ detection.

Cell Lines and Culture Conditions. SK–BR-3 ($HER2^+$) and MDA–MB-231 (HER2-) cells were obtained from the American Type Culture Collection (ATCC, HTB-30, and HTB-26, respectively). Cells were grown in plastic culture flasks) at 37 °C in a humidified atmosphere of 5% CO_2. SK–BR-3 cells were cultured in McCoy's 5a Medium Modified and MDA–MB-231 cells in Dulbecco's Modified Eagle's Medium (DMEM), both supplemented with 10% heat-inactivated FBS and 1% penicillin/streptomycin. A subcultivation ratio of 1:2 was adopted to SK–BR-3 cells and 1:6 to MDA–MB-231 cells.

Antibody Bioconjugation. Bioconjugation reactions proceeded as follows: 25 equiv of **CA–TCO** in DMF (5%) were added to a 13 μM THIOMAB solution in Tris-HCl buffer (20 mM, pH 8.0) and allowed to react for 2 h at 37 °C with shaking (500 rpm). An aliquot was removed and 20 equiv of TCEP in Tris-HCl buffer (20 mM, pH 8.0) were added for 10 min at room temperature (RT) with shaking (500 rpm). The mixture was centrifuged at 16 900*g* for 2 min and analyzed by LC–MS. For the confocal microscopy and flow cytometry studies, the antibody was dialyzed for 18–20 h at 4 °C, using a Slide-A-Lyzer MINI Dialysis Device with a 10K molecular weight cutoff in Tris-HCl buffer (20 mM, pH 8.0) with at least one buffer exchange. For the radiolabeling and cellular uptake studies, the antibody was purified by ultrafiltration using Amicon Ultra-0.5 centrifugal filter devices with a 50K molecular weight cutoff, according to the manufacturer's protocol.

Click Reaction with Fluorescent Tetrazine. Thirty equiv of 6-methyl-tetrazine-sulfo-Cy3 (Jena Biosciences) in H_2O were added to a 13 μM solution of THIOMAB–TCO in Tris-HCl buffer (20 mM, pH 8.0). The reaction was incubated for 30 min at 37 °C with shaking (500 rpm).

Sodium Dodecyl Sulfate-Polyacrylamide Gel Electrophoresis. SDS-PAGE analysis was performed under reducing conditions. Samples were diluted in 4× NuPAGE LDS Sample Buffer (ThermoFisher Scientific) and 2-mercaptoethanol was added as reducing agent (10× solution). Samples were heated at 95 °C for 10 min, and loaded to a NuPAGE Bis-Tris gel (4–12% gradient). Electrophoresis proceeded at 200 V in 1× SDS Running Buffer (20× NuPAGE MES SDS Running Buffer pH 7.3). The gel was stained overnight at RT with a 0.5% (v/v) SYPRO Ruby solution for protein detection. Fluorescence was detected in a Amersham Typhoon imager (GE Healthcare Life Sciences).

Confocal Microscopy. Microscopy studies were performed on μ-Slide 8-well polymer coverslips chamberslides. SK–BR-3 and MDA–MB-231 cells were harvested with 1× TrypLE Express Enzyme, seeded at a density of 3.0 × 10^4 cells per well in complete culture medium, and allowed to adhere overnight at 37 °C and 5% CO_2. On the following day, culture medium was removed and cells were incubated for 45 min at 37 °C with THIOMAB or THIOMAB–TCO (0.75 μM) in complete medium. After antibody incubation, medium was removed, cells were washed with fresh medium, and incubated for 30 min at 37 °C with 6-methyl-tetrazine-sulfo-Cy3 solution in complete medium (29 μM, 38.5 equiv). After tetrazine incubation, cells were washed two times with PBS, and Hoechst 33342 (10 μg/mL) was added for 5 min at RT. Cells were then washed three times with PBS, and fixed with 4% paraformaldehyde in PBS for 15 min at RT. Cells were further

https://dx.doi.org/10.1021/acs.bioconjchem.0c00551
Bioconjugate Chem. 2021, 32, 121–132

washed two times with PBS, and covered in mounting medium. Blocking studies were performed in SK−BR-3 cells by preincubating cells with THIOMAB (0.75 μM in complete medium) before treatment with THIOMAB−TCO. Fluorescence microscopy was performed using a Zeiss LSM 880 inverted microscope, using 405 nm laser excitation for Hoechst and 488 nm laser excitation for Cy3. Identical image acquisition settings were used for experimental, control, and blocking data sets. Data was analyzed using the Fiji-ImageJ software.

Flow Cytometry. SK-BR-3 and MDA-MB-231 cells were harvested with TrypLE Express Enzyme, and 5.0×10^5 cells were collected, pelleted by centrifugation, and resuspended in a solution of THIOMAB or THIOMAB−TCO (0.75 μM in 3% (w/v) BSA/PBS). After 45 min at RT, cells were pelleted, washed two times with 3% BSA/PBS, and resuspended in 6-methyl-tetrazine-Sulfo-Cy3 solution in 3% BSA/PBS (29 μM, 38.5 equiv). After 30 min at 37 °C in the dark, cells were pelleted, washed two times with 3% BSA/PBS, and resuspended in 1% (w/v) BSA/PBS containing 5 mM EDTA. All centrifugation steps were performed at 300*g* for 5 min. Blocking studies were performed in SK−BR-3 cells by preincubating cells with THIOMAB (0.75 μM in 3% BSA/PBS) for 45 min at RT before incubation with THIOMAB−TCO. A negative, unstained control was included for each cell line to determine the level of intrinsic cell autofluorescence. Acquisition was performed on a BD Accuri C6 flow cytometer (BD Biosciences) set up with a 488 nm laser and the tetramethylrhodamine filter. Only results for single-cell events are shown. Data were analyzed using the FlowJo X 10 software.

Radiolabeling Studies. Labeling of DOTA−Tz with ^{111}In was performed as follows: to a vial already containing 7.4 to 30 MBq of $^{111}InCl_3$ (Curium), DOTA−Tz to a final concentration of 1×10^{-4} M, in 0.1 M ammonium acetate buffer pH 7, followed by incubation at 80 °C for 15 min. The resulting labeling yields were between 61 and 85%. ^{111}In−DOTA−Tz was purified by RP−HPLC and recovered in 0.1 M phosphate buffer pH 8 and obtained with >95% of RCP, as assessed by RP−HPLC and iTLC. The RCY was between 44 and 56%. Activities were measured in a dose calibrator (Capintec CRC-55tW, Mirion Technologies).

Labeling of TCO-modified THIOMAB with ^{111}In was accomplished through reaction of THIOMAB−TCO (13 μM) in Tris-HCl buffer (20 mM, pH 8.0) with the purified ^{111}In−DOTA−Tz (~7.4 MBq) at 37 °C. The reaction was monitored by iTLC, γ-detection. The clicked antibody conjugate was purified by ultrafiltration using Amicon Ultra-0.5 centrifugal filter devices with a 50K molecular weight cutoff, according to the manufacturer's protocol (final solution in 20 mM Tris-HCl buffer pH 8.0).

In Vitro Stability of ^{111}In-Labeled Antibody. Stability studies were performed in cell culture medium (DMEM + 10% FBS) and human serum. In addition, transchelation was assessed in the presence of an excess of diethylenetriamine-pentaacetic acid (DTPA) (0.1 M solution in ammonium acetate buffer pH 5). In general, the radiolabeled antibody was incubated at 37 °C with a 5-fold volume of each solution. Aliquots were removed at different time points and analyzed by iTLC. Data were expressed as a percentage of activity associated with clicked antibody at a given time point normalized to the activity associated with clicked antibody at 0 h of incubation.

Radioactive Cellular Uptake Studies. Cellular uptake studies were performed in 24-well tissue culture plates with SK−BR-3 and MDA−MB-231 cells seeded, respectively, at a density of 2.0×10^5 and 1.25×10^5 cells per well in complete culture medium. The assays were perfomed on the following day. For the cellular uptake of ^{111}In-labeled antibody, on the day of the assay, the cell medium was removed and cells were incubated with ^{111}In−DOTA−Tz−TCO−THIOMAB in complete medium (~18.5 kBq in 500 μL per well) at 37 °C. The medium containing the radioactive antibody was removed at different time points, and cells were washed twice with ice-cold PBS and lysed with 1 M NaOH for 10 min at 37 °C. For the cellular uptake with pretargeting strategy, on the day of the assay, cell medium was removed and cells were incubated with THIOMAB−TCO (25 nM) in complete medium for 45 min at 37 °C. Cells were washed with medium and incubated with ^{111}In−DOTA−Tz in complete medium (~18.5 kBq in 500 μL per well). At different time points, the medium containing the radioactive tetrazine was removed, and the cells were washed twice with ice-cold PBS and lysed with 1 M NaOH for 10 min at 37 °C. Cellular uptake of the radiolabeled tetrazine was assessed by cell incubation with ^{111}In−DOTA−Tz only. Blocking studies were also performed by previous incubation with unmodified THIOMAB (25 nM) in complete medium for 45 min at 37 °C. In the end the experiment, radioactivity added to the cells and in the lysates was measured in a γ-counter (Berthold-LB 211, Berthold Technologies). The assays were performed with 3−4 replicates for each time point. Cellular uptake values were expressed as a percentage of total activity added to cells normalized per million of cells ± standard deviation. Statistical analysis was performed with *t*-test for the clicked antibody and with two-way ANOVA for the pretargeting strategy, with a *p*-value <0.05 considered as the level of statistical significance in both cases.

In Vivo Studies. The animal studies were executed in laboratory animal facilities under the supervision of researchers accredited by the National Authorities and with the research project approved by the local ethical committee and the National Authority. Experiments were performed in compliance with the National and European Union directives regarding ethics, care, and protection of animals used for experimental and other scientific purposes. Biodistribution of ^{111}In−DOTA−Tz following pretargeting with THIOMAB−TCO was performed in female athymic nude mice (*Foxn1^{nu}*, Charles River). Animals were housed in an aseptic environment with controlled temperature (~24 °C) and humidity, following a 12 h light/12 h dark schedule and maintained on a normal diet ad libitum. Mice were distributed in two groups for SK-BR-3 xenografts (n = 3−4) and one group for MDA−MB-231 xenografts (n = 3). Each mouse (16-weeks old, ~28−30 g) was subcutaneously injected in the right flank with 150 μL of a 50:50 (v:v) Matrigel/FBS suspension containing $\sim 10 \times 10^6$ freshly harvested SK−BR-3 or MDA−MB-231 cells. Water supplemented with 17-β-estradiol (0.67 μg/mL) was given to animals inoculated with SK−BR-3 cells and changed twice per week, and an estradiol-containing pomade was also applied at the inoculation site every day. Tumor growth was determined by measurement of tumors using calipers twice a week. Volume of spheroid SK−BR-3 tumors ranged between 100 and 200 mm^3 and was calculated using the formula $V = (4/3) \times \pi \times r^3$, where r represents the radius of the sphere. Volume of ellipsoid MDA−MB-231 tumors ranged between 500 and 700 mm^3 and was calculated using the formula $V = (\pi/6) \times L \times W^2$, where L

https://dx.doi.org/10.1021/acs.bioconjchem.0c00551
Bioconjugate Chem. 2021, 32, 121−132

and *W* represent the major and minor diameters, respectively. At day 12 after inoculation, tumor-bearing mice received an intravenous (iv) injection via the tail vein of THIOMAB−TCO or unmodified THIOMAB (control group) at a total dose of 5 mg/kg (∼100 μL/mouse). Animals were maintained in the temperature- and humidity-controlled room and, 24 h later, were iv injected in the tail vein with 2.8−4.1 MBq of ^{111}In−DOTA−Tz (∼100 μL/mouse). Animals were sacrificed 24 h postinjection of ^{111}In-labeled tetrazine (∼48 h after antibody injection) by cervical dislocation. The ID in the mouse and the activity remaining in the sacrificed animal were measured in a dose calibrator (Capintec CRC-55tW, Mirion Technologies), and the difference was assumed to be due to excretion. Tissues and organs of interest were dissected, rinsed to remove excess blood, weighted, and the activity measured in a γ-counter (Berthold-LB 211, Berthold Technologies). Tissue and organ uptakes were expressed as percentage of ID per gram of tissue or organ (% ID/g). For blood, bone, and muscle, the percentage of ID/g was estimated assuming that these tissues represent, respectively, 6, 10, and 40% of the total body weight. Statistical analysis was performed with two-way ANOVA, with *p*-value <0.05 considered as the level of statistical significance.

■ ASSOCIATED CONTENT

Supporting Information

The Supporting Information is available free of charge at https://pubs.acs.org/doi/10.1021/acs.bioconjchem.0c00551.

Figures S1−S11, LC−MS, SE−HPLC, SDS-PAGE, confocal imaging, and flow cytometry data for THIOMAB and THIOMAB−TCO; Figures S12−S17, iTLC analysis, in vitro stability, uptake, and renal excretion data for ^{111}In−DOTA−TZ−TCO−THIOMAB; Table S1, biodistribution and renal excretion data for ^{111}In−DOTA−TZ−TCO−THIOMAB; and additional experimental details (PDF)

■ AUTHOR INFORMATION

Corresponding Authors

Filipa Mendes − *Center for Nuclear Sciences and Technologies (C2TN), Instituto Superior Técnico and Departamento de Engenharia e Ciências Nucleares (DECN), Instituto Superior Técnico, Universidade de Lisboa, 2695-066 Bobadela LRS, Portugal;* orcid.org/0000-0003-0646-1687; Email: fmendes@ctn.tecnico.ulisboa.pt

Gonçalo J. L. Bernardes − *Instituto de Medicina Molecular João Lobo Antunes (iMM-JLA), Faculdade de Medicina, Universidade de Lisboa, 1649-028 Lisboa, Portugal; Department of Chemistry, University of Cambridge, CB2 1EW Cambridge, United Kingdom;* orcid.org/0000-0001-6594-8917; Email: gb453@cam.ac.uk

Bruno L. Oliveira − *Instituto de Medicina Molecular João Lobo Antunes (iMM-JLA), Faculdade de Medicina, Universidade de Lisboa, 1649-028 Lisboa, Portugal;* Email: bruno.oliveira@medicina.ulisboa.pt

Authors

Vera F. C. Ferreira − *Center for Nuclear Sciences and Technologies (C2TN), Instituto Superior Técnico, Universidade de Lisboa, 2695-066 Bobadela LRS, Portugal*

Alice D'Onofrio − *Center for Nuclear Sciences and Technologies (C2TN), Instituto Superior Técnico, Universidade de Lisboa, 2695-066 Bobadela LRS, Portugal;* orcid.org/0000-0001-6740-8607

Carlos M. Farinha − *Biosystems and Integrative Sciences Institute (BioISI), Faculdade de Ciências, Universidade de Lisboa, 1749-016 Lisboa, Portugal*

Lurdes Gano − *Center for Nuclear Sciences and Technologies (C2TN), Instituto Superior Técnico and Departamento de Engenharia e Ciências Nucleares (DECN), Instituto Superior Técnico, Universidade de Lisboa, 2695-066 Bobadela LRS, Portugal*

António Paulo − *Center for Nuclear Sciences and Technologies (C2TN), Instituto Superior Técnico and Departamento de Engenharia e Ciências Nucleares (DECN), Instituto Superior Técnico, Universidade de Lisboa, 2695-066 Bobadela LRS, Portugal*

Complete contact information is available at: https://pubs.acs.org/10.1021/acs.bioconjchem.0c00551

Notes

With regard to this publication, G.J.L.B. has received research reagents from Genentech.

The authors declare no competing financial interest.

■ ACKNOWLEDGMENTS

This work is funded by Fundação para a Ciência e Tecnologia−FCT (PTDC/BTM-TEC/29256/2017 (co-funded by Lisboa2020−EU FEDER to F.M.) and UID/Multi/04349/2019). V.F.C.F. also acknowledges FCT for the PhD fellowship (SFRH/BD/108623/2015) and the Federation of European Biochemical Societies for a Summer Fellowship. Funding is also acknowledged to the Royal Society (URF to G.J.L.B., URF/R/180019) and FCT Portugal (iFCT to G.J.L.B., IF/00624/2015 and FCT Stimulus to B.L.O., CEECIND/02335/2017). This project has received funding from the European Union's Horizon 2020 research and innovation programme under grant agreements 807281, 702428, and 852985. The authors would like to thank Dr Célia Fernandes (C^{2}TN) for fruitful discussions and Elisabete Correia (C^{2}TN) for excellent technical support.

■ REFERENCES

(1) Warram, J. M., de Boer, E., Sorace, A. G., Chung, T. K., Kim, H., Pleijhuis, R. G., van Dam, G. M., and Rosenthal, E. L. (2014) Antibody-based imaging strategies for cancer. *Cancer Metastasis Rev. 33* (2−3), 809−822.

(2) Dammes, N., and Peer, D. (2020) Monoclonal antibody-based molecular imaging strategies and theranostic opportunities. *Theranostics 10* (2), 938−955.

(3) Freise, A. C., and Wu, A. M. (2015) In vivo imaging with antibodies and engineered fragments. *Mol. Immunol. 67* (2), 142−152.

(4) Garousi, J., Orlova, A., Frejd, F. Y., and Tolmachev, V. (2020) Imaging using radiolabelled targeted proteins: radioimmunodetection and beyond. *EJNMMI radiopharm. Chem. 5* (1), 16−16.

(5) Reardan, D. T., Meares, C. F., Goodwin, D. A., McTigue, M., David, G. S., Stone, M. R., Leung, J. P., Bartholomew, R. M., and Frincke, J. M. (1985) Antibodies against metal chelates. *Nature 316* (6025), 265−268.

(6) Hnatowich, D. J., Virzi, F., and Rusckowski, M. (1987) Investigations of avidin and biotin for imaging applications. *J. Nucl. Med. 28* (8), 1294−1302.

(7) Knight, J. C., and Cornelissen, B. (2014) Bioorthogonal chemistry: implications for pretargeted nuclear (PET/SPECT) imaging and therapy. *Nucl. Med. Mol. Imaging 4* (2), 96−113.

(8) Altai, M., Membreno, R., Cook, B., Tolmachev, V., and Zeglis, B. M. (2017) Pretargeted Imaging and Therapy. *J. Nucl. Med. 58* (10), 1553−1559.
(9) Oliveira, B. L., Guo, Z., and Bernardes, G. J. L. (2017) Inverse electron demand Diels-Alder reactions in chemical biology. *Chem. Soc. Rev. 46* (16), 4895−4950.
(10) Devaraj, N. K. (2018) The Future of Bioorthogonal Chemistry. *ACS Cent. Sci. 4* (8), 952−959.
(11) Rondon, A., and Degoul, F. (2020) Antibody Pretargeting Based on Bioorthogonal Click Chemistry for Cancer Imaging and Targeted Radionuclide Therapy. *Bioconjugate Chem. 31* (2), 159−173.
(12) Blackman, M. L., Royzen, M., and Fox, J. M. (2008) Tetrazine ligation: fast bioconjugation based on inverse-electron-demand Diels-Alder reactivity. *J. Am. Chem. Soc. 130* (41), 13518−13519.
(13) Garcia, M. F., Gallazzi, F., Junqueira, M. S., Fernandez, M., Camacho, X., Mororo, J. D. S., Faria, D., Carneiro, C. G., Couto, M., Carrion, F., Pritsch, O., Chammas, R., Quinn, T., Cabral, P., and Cerecetto, H. (2018) Synthesis of hydrophilic HYNIC-[1,2,4,5]-tetrazine conjugates and their use in antibody pretargeting with (99m)Tc. *Org. Biomol. Chem. 16* (29), 5275−5285.
(14) Mandikian, D., Rafidi, H., Adhikari, P., Venkatraman, P., Nazarova, L., Fung, G., Figueroa, I., Ferl, G. Z., Ulufatu, S., Ho, J., McCaughey, C., Lau, J., Yu, S. F., Prabhu, S., Sadowsky, J., and Boswell, C. A. (2018) Site-specific conjugation allows modulation of click reaction stoichiometry for pretargeted SPECT imaging. *MAbs 10* (8), 1269−1280.
(15) Rossin, R., Verkerk, P. R., van den Bosch, S. M., Vulders, R. C., Verel, I., Lub, J., and Robillard, M. S. (2010) In vivo chemistry for pretargeted tumor imaging in live mice. *Angew. Chem., Int. Ed. 49* (19), 3375−3378.
(16) Zeglis, B. M., Sevak, K. K., Reiner, T., Mohindra, P., Carlin, S. D., Zanzonico, P., Weissleder, R., and Lewis, J. S. (2013) A pretargeted PET imaging strategy based on bioorthogonal Diels-Alder click chemistry. *J. Nucl. Med. 54* (8), 1389−1396.
(17) Houghton, J. L., Zeglis, B. M., Abdel-Atti, D., Sawada, R., Scholz, W. W., and Lewis, J. S. (2016) Pretargeted Immuno-PET of Pancreatic Cancer: Overcoming Circulating Antigen and Internalized Antibody to Reduce Radiation Doses. *J. Nucl. Med. 57* (3), 453−459.
(18) Cook, B. E., Adumeau, P., Membreno, R., Carnazza, K. E., Brand, C., Reiner, T., Agnew, B. J., Lewis, J. S., and Zeglis, B. M. (2016) Pretargeted PET Imaging Using a Site-Specifically Labeled Immunoconjugate. *Bioconjugate Chem. 27* (8), 1789−1795.
(19) Billaud, E. M. F., Belderbos, S., Cleeren, F., Maes, W., Van de Wouwer, M., Koole, M., Verbruggen, A., Himmelreich, U., Geukens, N., and Bormans, G. (2017) Pretargeted PET Imaging Using a Bioorthogonal (18)F-Labeled trans-Cyclooctene in an Ovarian Carcinoma Model. *Bioconjugate Chem. 28* (12), 2915−2920.
(20) Keinanen, O., Fung, K., Pourat, J., Jallinoja, V., Vivier, D., Pillarsetty, N. K., Airaksinen, A. J., Lewis, J. S., Zeglis, B. M., and Sarparanta, M. (2017) Pretargeting of internalizing trastuzumab and cetuximab with a (18)F-tetrazine tracer in xenograft models. *EJNMMI Res. 7* (1), 95−98.
(21) Ruivo, E., Elvas, F., Adhikari, K., Vangestel, C., Van Haesendonck, G., Lemiere, F., Staelens, S., Stroobants, S., Van der Veken, P., Wyffels, L., and Augustyns, K. (2020) Preclinical Evaluation of a Novel (18)F-Labeled dTCO-Amide Derivative for Bioorthogonal Pretargeted Positron Emission Tomography Imaging. *ACS Omega 5* (9), 4449−4456.
(22) Evans, H. L., Nguyen, Q. D., Carroll, L. S., Kaliszczak, M., Twyman, F. J., Spivey, A. C., and Aboagye, E. O. (2014) A bioorthogonal (68)Ga-labelling strategy for rapid in vivo imaging. *Chem. Commun. 50* (67), 9557−9560.
(23) Meyer, J.-P., Houghton, J. L., Kozlowski, P., Abdel-Atti, D., Reiner, T., Pillarsetty, N. V. K., Scholz, W. W., Zeglis, B. M., and Lewis, J. S. (2016) 18F-Based Pretargeted PET Imaging Based on Bioorthogonal Diels−Alder Click Chemistry. *Bioconjugate Chem. 27* (2), 298−301.
(24) Edem, P. E., Jorgensen, J. T., Norregaard, K., Rossin, R., Yazdani, A., Valliant, J. F., Robillard, M., Herth, M. M., and Kjaer, A. (2020) Evaluation of a (68)Ga-Labeled DOTA-Tetrazine as a PET Alternative to (111)In-SPECT Pretargeted Imaging. *Molecules 25* (3), 463−477.
(25) Hoyt, E. A., Cal, P. M. S. D., Oliveira, B. L., and Bernardes, G. J. L. (2019) Contemporary approaches to site-selective protein modification. *Nature Rev. Chem. 3*, 147−171.
(26) Chalker, J. M., Bernardes, G. J., Lin, Y. A., and Davis, B. G. (2009) Chemical modification of proteins at cysteine: opportunities in chemistry and biology. *Chem. - Asian J. 4* (5), 630−640.
(27) Ochtrop, P., and Hackenberger, C. P. R. (2020) Recent advances of thiol-selective bioconjugation reactions. *Curr. Opin. Chem. Biol. 58*, 28−36.
(28) Baldwin, A. D., and Kiick, K. L. (2011) Tunable Degradation of Maleimide−Thiol Adducts in Reducing Environments. *Bioconjugate Chem. 22* (10), 1946−1953.
(29) Cal, P. M., Bernardes, G. J., and Gois, P. M. (2014) Cysteine-selective reactions for antibody conjugation. *Angew. Chem., Int. Ed. 53* (40), 10585−10587.
(30) Ravasco, J. M. J. M., Faustino, H., Trindade, A., and Gois, P. M. P. (2019) Bioconjugation with Maleimides: A Useful Tool for Chemical Biology. *Chem. - Eur. J. 25* (1), 43−59.
(31) Bernardim, B., Cal, P. M., Matos, M. J., Oliveira, B. L., Martinez-Saez, N., Albuquerque, I. S., Perkins, E., Corzana, F., Burtoloso, A. C., Jimenez-Oses, G., and Bernardes, G. J. (2016) Stoichiometric and irreversible cysteine-selective protein modification using carbonylacrylic reagents. *Nat. Commun. 7* (1), 13128−13132.
(32) Bernardim, B., Matos, M. J., Ferhati, X., Compañón, I., Guerreiro, A., Akkapeddi, P., Burtoloso, A. C. B., Jiménez-Osés, G., Corzana, F., and Bernardes, G. J. L. (2019) Efficient and irreversible antibody−cysteine bioconjugation using carbonylacrylic reagents. *Nat. Protoc. 14* (1), 86−99.
(33) Junutula, J. R., Raab, H., Clark, S., Bhakta, S., Leipold, D. D., Weir, S., Chen, Y., Simpson, M., Tsai, S. P., Dennis, et al. (2008) Site-specific conjugation of a cytotoxic drug to an antibody improves the therapeutic index. *Nat. Biotechnol. 26* (8), 925−932.
(34) Dijkers, E. C., Oude Munnink, T. H., Kosterink, J. G., Brouwers, A. H., Jager, P. L., de Jong, J. R., van Dongen, G. A., Schröder, C. P., Lub-de Hooge, M. N., and de Vries, E. G. (2010) Biodistribution of 89Zr-trastuzumab and PET Imaging of HER2-Positive Lesions in Patients With Metastatic Breast Cancer. *Clin. Pharmacol. Ther. 87* (5), 586−592.
(35) Holloway, C. M. B., Scollard, D. A., Caldwell, C. B., Ehrlich, L., Kahn, H. J., and Reilly, R. M. (2013) Phase I trial of intraoperative detection of tumor margins in patients with HER2-positive carcinoma of the breast following administration of 111In-DTPA-trastuzumab Fab fragments. *Nucl. Med. Biol. 40* (5), 630−637.
(36) Sandstrom, M., Lindskog, K., Velikyan, I., Wennborg, A., Feldwisch, J., Sandberg, D., Tolmachev, V., Orlova, A., Sorensen, J., Carlsson, J., Lindman, H., and Lubberink, M. (2016) Biodistribution and Radiation Dosimetry of the Anti-HER2 Affibody Molecule 68Ga-ABY-025 in Breast Cancer Patients. *J. Nucl. Med. 57* (6), 867−71.
(37) Ulaner, G. A., Lyashchenko, S. K., Riedl, C., Ruan, S., Zanzonico, P. B., Lake, D., Jhaveri, K., Zeglis, B., Lewis, J. S., and O'Donoghue, J. A. (2018) First-in-Human Human Epidermal Growth Factor Receptor 2-Targeted Imaging Using (89)Zr-Pertuzumab PET/CT: Dosimetry and Clinical Application in Patients with Breast Cancer. *J. Nucl. Med. 59* (6), 900−906.
(38) Pereira, P. M. R., Abma, L., Henry, K. E., and Lewis, J. S. (2018) Imaging of human epidermal growth factor receptors for patient selection and response monitoring - From PET imaging and beyond. *Cancer Lett. 419*, 139−151.
(39) Nazarova, L., Rafidi, H., Mandikian, D., Ferl, G. Z., Koerber, J. T., Davies, C. W., Ulufatu, S., Ho, J., Lau, J., Yu, S. F., Ernst, J., Sadowsky, J. D., and Boswell, C. A. (2020) Effect of Modulating FcRn Binding on Direct and Pretargeted Tumor Uptake of Full-length Antibodies. *Mol. Cancer Ther. 19* (4), 1052−1058.
(40) Mandleywala, K., Shmuel, S., Pereira, P. M. R., and Lewis, J. S. (2020) Antibody-Targeted Imaging of Gastric Cancer. *Molecules 25* (20), 4621−4633.

https://dx.doi.org/10.1021/acs.bioconjchem.0c00551
Bioconjugate Chem. 2021, 32, 121−132

(41) Ren, W., Liu, Y., Wan, S., Fei, C., Wang, W., Chen, Y., Zhang, Z., Wang, T., Wang, J., Zhou, L., Weng, Y., He, T., and Zhang, Y. (2014) BMP9 Inhibits Proliferation and Metastasis of HER2-Positive SK-BR-3 Breast Cancer Cells through ERK1/2 and PI3K/AKT Pathways. *PLoS One 9* (5), e96816.
(42) D'Onofrio, A., Paulo, A., Gano, L., Oliveira, C., Mendes, F., Dunn, S., and Fierle, J. (2018) Towards clickable radioimmunoconjugates as theranostic agents for TEM1 targeting. *Mol. Imag. Biol. 20* (S1), 1−584.
(43) Austin, C. D., De Maziere, A. M., Pisacane, P. I., van Dijk, S. M., Eigenbrot, C., Sliwkowski, M. X., Klumperman, J., and Scheller, R. H. (2004) Endocytosis and sorting of ErbB2 and the site of action of cancer therapeutics trastuzumab and geldanamycin. *Mol. Biol. Cell 15* (12), 5268−82.
(44) Ram, S., Kim, D., Ober, R. J., and Ward, E. S. (2014) The level of HER2 expression is a predictor of antibody-HER2 trafficking behavior in cancer cells. *MAbs 6* (5), 1211−1219.
(45) Ovacik, M., and Lin, K. (2018) Tutorial on Monoclonal Antibody Pharmacokinetics and Its Considerations in Early Development. *Clin. Transl. Sci. 11* (6), 540−552.
(46) Rossin, R., Läppchen, T., van den Bosch, S. M., Laforest, R., and Robillard, M. S. (2013) Diels−Alder Reaction for Tumor Pretargeting: In Vivo Chemistry Can Boost Tumor Radiation Dose Compared with Directly Labeled Antibody. *J. Nucl. Med. 54* (11), 1989−1995.
(47) Meyer, J.-P., Tully, K. M., Jackson, J., Dilling, T. R., Reiner, T., and Lewis, J. S. (2018) Bioorthogonal Masking of Circulating Antibody−TCO Groups Using Tetrazine-Functionalized Dextran Polymers. *Bioconjugate Chem. 29* (2), 538−545.
(48) Pereira, P. M. R., Sharma, S. K., Carter, L. M., Edwards, K. J., Pourat, J., Ragupathi, A., Janjigian, Y. Y., Durack, J. C., and Lewis, J. S. (2018) Caveolin-1 mediates cellular distribution of HER2 and affects trastuzumab binding and therapeutic efficacy. *Nat. Commun. 9* (1), 5137−5151.
(49) Pereira, P. M. R., Mandleywala, K., Ragupathi, A., Carter, L. M., Goos, J., Janjigian, Y. Y., and Lewis, J. S. (2019) Temporal Modulation of HER2Membrane Availability Increases Pertuzumab Uptake and Pretargeted Molecular Imaging of Gastric Tumors. *J. Nucl. Med. 60* (11), 1569−1578.
(50) Hommelgaard, A. M., Lerdrup, M., and van Deurs, B. (2004) Association with membrane protrusions makes ErbB2 an internalization-resistant receptor. *Mol. Biol. Cell 15* (4), 1557−1567.
(51) Pereira, P. M. R., Mandleywala, K., Ragupathi, A., and Lewis, J. S. (2020) Acute Statin Treatment Improves Antibody Accumulation in EGFR- and PSMA-Expressing Tumors. *Clin. Cancer Res. 26*, 6215.

https://dx.doi.org/10.1021/acs.bioconjchem.0c00551
Bioconjugate Chem. 2021, 32, 121−132